Local effects of immunosuppressants in the skin and impact on UV carcinogenesis

Voskamp, P.

Chapter 3

Rapamycin impairs UV induction of mutant-p53 overexpressing cell clusters without affecting tumor onset

Voskamp P, Bodmann CA, Rebel HG, Koehl GE, Tensen CP, Bouwes Bavinck JN, El Ghalbzouri A, Van Kranen HJ, Willemze R, Geissler EK, De Gruijl FR

Int J Cancer. 2011 Dec 9. doi: 10.1002/ijc.27391. [Epub ahead of print]

Abstract

Because of its anti-tumor effect, the immunosuppressant rapamycin holds great promise for organ transplant recipients in that it may lower their cancer risk. In a mouse model we showed previously that rapamycin inhibits the outgrowth of primary skin carcinomas induced by UV radiation. However, the tumors that did grow out showed an altered *p53* mutation spectrum. Here, we investigated whether this shift in *p53* mutations already occurred in the smallest tumors, which were not affected in onset. We found that rapamycin did not alter the mutational spectrum in small tumors and in preceding microscopic clusters of cells expressing mutant-p53. However, rapamycin did reduce the number of these cell clusters. As this reduction did not affect tumor onset, we subsequently investigated whether rapamycin merely suppressed expression of mutated p53. This was not the case, as we could demonstrate that switching from a diet with rapamycin to one without, or vice versa, did not affect the number of existing mutant-p53 expressing cell clusters. Hence, rapamycin actually reduced the formation of mutant-p53 cell clusters. In wild-type and p53-mutant mice we could not measure a significant enhancement of UV-induced apoptosis, but we did observe clear enhancement in human skin equivalents. This was associated with a clear suppression of HIF1α accumulation. Thus, we conclude that rapamycin reduces the formation of mutant-p53-expressing cell clusters without affecting tumor onset, suggesting that tumors grow out of a minor subset of cell clusters, the formation of which is not affected by rapamycin.

Introduction

Organ transplant recipients have a high incidence of skin cancers. An important risk factor for skin cancer development appears to be immunosuppressive therapy, especially when the conventional immunosuppressants cyclosporine and azathioprine are used[1, 2]. The immunosuppressive drug rapamycin (sirolimus) has now been used for several years in immunosuppressive therapies in organ transplant recipients and appears promising in reducing the post-transplant cancer risk[3].

Rapamycin is an immunosuppressant that exerts its effect through inhibition of the mammalian target of rapamycine (mTOR) pathway, which is a mechanism of action entirely different from that of other immunosuppressants. Rapamycin has been shown to inhibit the mTORC1 complex, preventing p70s6k from becoming activated and thereby preventing S6 phosphorylation and by inhibiting 4EBP1, both processes affecting protein synthesis differently[4]. Furthermore, rapamycin has been shown to inhibit hypoxia-induced HIF1α and VEGF expression[5]. HIF1α accumulates in nuclei of keratinocytes after UV irradiation in a biphasic manner, peaking in protein expression at 10-24 hours after irradiation[6]. Rapamycin increased apoptosis in murine embryo fibroblasts deficient in p53 after serum depletion, while infection with Ad-p53 completely protected against rapamycin-induced apoptosis by inducing G1 cell cycle arrest[7].

Recent studies indicate that rapamycin decreases the rate at which skin malignancies develop. A switch to rapamycin therapy in a small study reduced the development of (pre) malignancies and nonmelanoma skin cancer in renal transplant patients[3]. Studies using hairless mice have also shown inhibiting effects of rapamycin on tumors; it reduced the incidence and progression of UV-induced skin cancer[8]. In a previous study by our group rapamycin did not affect the onset of UV-induced skin tumors <1mm, but showed decreased numbers of tumors >2mm (chapter 2). The latter study also showed that UV-induced tumors >2mm from rapamycin-fed mice harbor a different mutational spectrum of the *p53* gene, with less UV signature mutations (i.e. C to T transitions at dipyrimidine sites), compared with tumors from control-fed mice.

Hence, rapamycin does not affect tumor onset but it decreases development of large tumors, indicating that a specific subset of small tumors is not inhibited in growth by rapamycin. Increased levels of reactive oxygen species have been described in yeast to inhibit binding of rapamycin to its target TORC1, leading to rapamycin insensitivity[10]. The mechanism for rapamycin insensitivity may thus be linked to the altered *p53* mutational spectrum. This

led us to the hypothesis that the altered *p53* mutational spectrum occurs late in tumor development and is not present in the majority of small tumors or precursor lesions. UV-induced skin tumors >2mm typically harbor multiple *p53* mutations (chapter 2). The altered mutational spectrum may therefore appear late in tumor development without affecting tumor onset which is associated with early *p53* mutations, or a minor subset with deviant *p53* mutations may escape inhibition by rapamycin early-on in tumor development. To test this hypothesis on a shift in types of *p53* mutations we have determined *p53* mutations in tumors <2mm and clusters of mutant-p53 overexpressing cells (mut-p53 cell clusters) which arise in the skin after repeated UV exposure and are generally regarded as skin tumor precursors[11-14].

In performing this experiment we found that the number of mut-p53 cell clusters was lower in rapamycin-fed mice than in control mice. The apparent discrepancy between the reduction in mut-p53 cell clusters and unaltered tumor onset led to the hypothesis that rapamycin either decreases expression of the p53 protein or acts in a pro-apoptotic manner on mut-p53 cell clusters. A possible effect on expression of mutant p53 was tested by switching between diets with and without rapamycin, which would also demonstrate whether any disappearance of mut-p53 cell clusters is associated with apoptosis. A possible effect on UV-induced apoptosis was further studied in (conditional) mutant(P275S) p53 knock-in mice and wild-type mice, and more extensively in human skin equivalents. In this investigation we have identified the disparate effects of rapamycin in successive stages of UV carcinogenesis, demonstrating that local effects in the skin culminating in mutant p53-expressing cell clusters need not be predictive of tumor onset.

Materials and methods

SKH1 mouse model

SKH-1 hairless mice (Charles River, Maastricht, The Netherlands) entered the experiment at 8-16 weeks of age; both male and female mice were used. The animal room was illuminated with yellow fluorescent tubes (Philips TL40W/16, Eindhoven, The Netherlands) that did not emit any measurable UV radiation. The animals were housed individually in Macrolon type 1 cages (Techniplast, Bugguggiate, Italy) under a 12 h light-12 h dark cycle at 23°C. Chow was supplied in ample amounts (55-60 g/mouse/week), and drinking water was available *ad libitum*. Cage enrichment was absent to prevent shielding of the animals from UV exposure. All experiments were performed in accordance with legislation and approval of the medical center's ethics committee.

Groups on diets with admixture of rapamycin

To avoid repeated i.p. injections rapamycin was admixed to standard mouse chow resulting in physiologically relevant blood levels as described previously (chapter 2). For the present experiment ssniff *GmbH* (Soest, Germany) supplied the chow with rapamycin at 20 mg/kg, which was stored in a cold room and renewed every month. A study was performed to determine the rapamycin blood levels after starting (t=0, 1, 2 and 3 days after start, n=7-15) and stopping (t=0, 1, 2, 3 and 7 days after stop, n=3-15) the rapamycin diet. Blood of the mice was taken retroorbially between 8 and 9 a.m., and was subsequently analyzed by the Department of Clinical Chemistry (University of Regensburg) by LC-MS/MS for rapamycin concentration. Two diet groups were formed: rapamycin (n=10) and a control group (n=16) fed the standard chow without admixtures. For 10 weeks the mice were kept on their assigned food, then, in some experiments, the groups switched foods, i.e. the rapamycin group was put on control food and vice versa. Before (t=0, n=4), and at different time points after switching food (t=1, 2, 3 and 7 days, n=3), mice were taken out of the experiment (figure 3A).

Mutant $p53^{P275S/+}$ mice

Because both in humans and mice the human codon 278 has been proven a UVB exposure specific mutational hotspot, we have selected the murine equivalent p53P275S mutant for this study. The generation of this conditional point mutant p53 strain of mice was essentially as described for two other p53 point mutant mice with the $p53^{R172H}$ allele and the $p53^{R270H}$ allele[15] and can be briefly summarized as follows. The P275S point mutated allele was constructed by site-directed mutagenesis as described before[16] and has been made conditional by the introduction of a LoxP-flanked transcriptional STOP cassette into intron 1 of the *p53* gene (figure 1). This Lox-STOP-Lox (LSL) cassette was kindly supplied by Dave Tuveson. Detailed characterization of the LSL cassette was provided elsewhere upon the creation of a conditional oncogenic allele of K-ras[17]. This conditional p53P275S allele (18.7 kb) was verified by sequencing the entire construct (data not shown) and targeted into Ola129(E14) embryonic stem cells. Germline transmission was achieved in multiple clones and the presence of the STOP cassette in intron 1 and the presence of the P275S point mutation of these mice was determined by PCR (data not shown). After >5 generations of backcrossing to a C57Bl6 background, $p53^{P275S/+}$ mice were crossbred with EIIa-Cre deleter mice (both strains acquired from the Department of Human Genetics, LUMC, Leiden) yielding offspring with a mutant *p53* allele (C>T mutation changing P to S in codon 275, the UV-mutational hotspot) and wild-type (wt) littermates. As this study is the first to use the mice carrying the $p53^{P275S}$ allele, we checked transcription of mutant

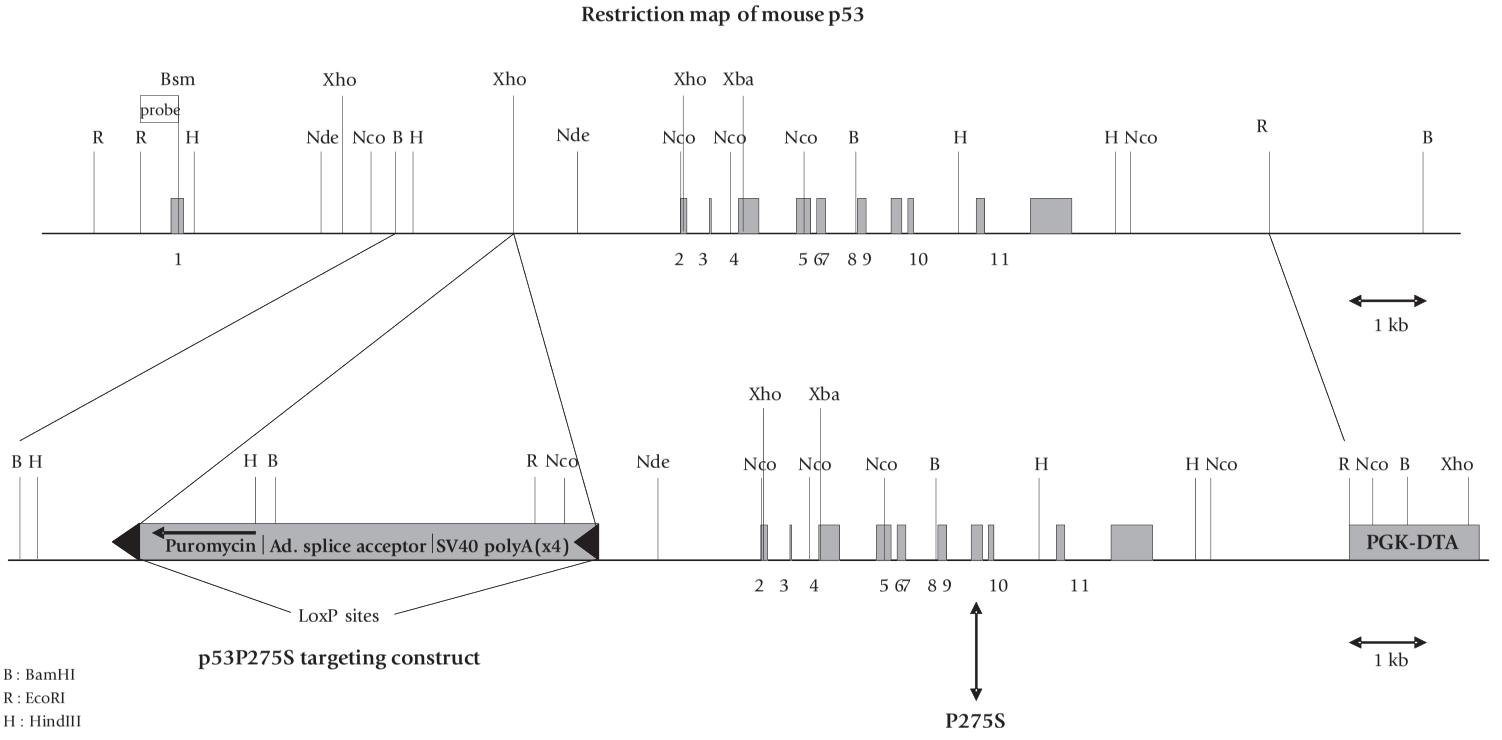

Figure 1: Generation of the p53P275S mutated allele. Insertion of the LoxSTOPLox cassette is shown. The PGK-DTA selection marker cassette was introduced during the construction of the point mutation in codon 275[16].

p53 mRNA in the EIIa-Cre/p53^{P275S} mice. The epidermises of F2 experimental animals were checked on expression of mutant p53 after UV exposure by staining with PAb240, excluding a minority (n=3) of mosaic mice not expressing mutant-p53 in the epidermis. Thus, twelve wt mice and eight mutant-p53 mice contributed to the final data. The mice were started on experimental diets (with or without rapamycin) for two weeks prior to UV irradiation. Mice were shaven one day prior to UV irradiation with 1.5MED (2250J/m^2) or 3MED (4500J/m^2). Forty-eight hours after irradiation mice were sacrificed and biopsies of the skin were taken. Part of each biopsy was snap-frozen in liquid nitrogen, with the other part being fixed in 4% formaldehyde, dehydrated and embedded in paraffin. Sections of the biopsies were stained for active caspase-3, p53 (CM5) and mutant p53 (Pab240).

Human Skin Equivalents (HSE)

Keratinocytes were isolated as described earlier[18]. In brief, surplus skin obtained from cosmetic surgery (obtained in accordance with the Dutch Law on Medical Treatment Agreement) was cut into small fragments and incubated overnight in dispase II (Roche Diagnostics, Almere, The Netherlands). Keratinocytes were isolated from the epidermis through incubation with trypsin at 37°C for 15 minutes. After trypsin inactivation, cells were filtered and cultured in keratinocyte medium at 37°C and 7.3% CO_2 until sub-confluency. Keratinocyte medium consisted of 3 parts Dulbecco's modified Eagle's medium (DMEM, Gibco/Invitrogen, Breda, The Netherlands) and 1 part Ham's F12 medium supplemented with 5% fetal bovine serum (FBS, HyClone/Greiner, Nürtingen, Germany), 0.5 mM hydrocortisone, 1 mM isoproterenol, 0.1 mM insulin (Sigma-Aldrich, Zwijndrecht, The Netherlands), 100 U ml^{-1} penicillin and 100 µg ml^{-1} streptomycin (Invitrogen, Breda, The Netherlands). For isolation of normal human dermal fibroblasts (NHDFs), human dermis was obtained by overnight incubation of fresh surplus skin from cosmetic surgery with dispase II. Fibroblasts were isolated from the dermis by incubation with a solution consisting of collagenase II (Invitrogen, Breda, The Netherlands) and dispase II (ratio 1:3) at 37°C for 2 hours. The cells were filtered, and cultured in fibroblast medium at 37°C and 5% CO_2 until sub-confluency. Fibroblast medium consisted of DMEM supplemented with 5% FBS, 100 U ml^{-1} penicillin and 100 µg ml^{-1} streptomycin. Passages 2-5 were used for the experiments.

Full-Thickness Models (FTM) using rat-tail collagen were generated as described before[18]. In brief, 80 x 10^3 fibroblasts were seeded into acetic acid extracted rat-tail collagen. The fibroblast-populated matrices were cultured for a week in standard fibroblast medium. FTMs were seeded with 50 x 10^4 normal human epidermal keratinocytes in low passage per model. Cultures were incubated overnight in keratinocyte medium supplemented with

1% FBS, 53µM selenious acid, 10mM L-serine, 10µM L-carnitine, 1mM dL-a-tocopherol-acetate, 100µg ml^{-1} ascorbic acid phosphate, 2.4 x 10^{-5} M bovine serum albumin and a lipid supplement containing 25mM palmitic acid, 15mM linoleic acid and 7mM arachidonic acid (Sigma-Aldrich, Zwijndrecht, The Netherlands). Culture medium was then replaced with supplemented keratinocyte medium as described above, except that serum was omitted and the concentration of linoleic acid was increased to 30 mM. The models were cultured air-exposed from this time onward. Medium was refreshed twice per week. After 2 weeks of air-exposed culture, the HSEs were processed for analysis.

Supplement/Chemicals

Rapamycin (Calbiochem, Canada) dissolved in absolute DMSO was supplemented to HSEs (0.1%) that were cultured for 11 days at the air-liquid interface. Rapamycin concentrations used were 10 or 100nM[19], and were applied two days prior to UV irradiation.

UV-source

Mice: Six groups were started on their respective diets 1 week before subjecting them to a regimen of daily UV exposure. TL-12/40W tubes (Philips, Eindhoven, The Netherlands; 54% output in UVB – 280 to 315 nm – and 46% output in UVA – 315 to 400 nm) were used for daily UV exposure. The lamps were mounted over the cages with grid covers to allow undisturbed exposure of the mice. The lamps were automatically switched on daily from 12.30 to 12.50 h. The threshold dose for a sunburn reaction (minimal edemal dose, MED) in the hairless SKH-1 mouse was ~500J/m^2 UV under these lamps. The lamps were dimmed both electronically and by insertion of perforated metal sheets to expose the mice daily to 250 J/m^2 of UV radiation (0.5 MED).

HSE: Skin models were exposed to UV irradiation from TL-12/20W tubes (Philips, Eindhoven, The Netherlands; 54% output in UVB – 280 to 315 nm – and 46% output in UVA – 315 to 400 nm) at 0.28 mJ/cm^2/sec. UV dosages ranged from 0 to 110 mJ/cm^2 of which the higher dosages yield significant apoptotic response.

Mutant-p53 immunostaining in epidermal sheets

Within 24 hrs after the last irradiation, mice were sacrificed and 11 × 34 mm pieces of dorsal skin were excised and treated with a thermolysin solution, after which the epidermal sheet was separated. A modified procedure of epidermal sheet preparation and subsequent immunostaining and analysis was used[12]. Pab240 antibody (Monosan) was used at a 1:250 dilution, with secondary goat anti-mouse-biotin antibody (Dako) used at a 1:200 dilution.

P53 mutation determination

RNA extracted from tumors <2mm was converted to cDNA and used as a template to amplify and subsequently sequence the entire coding sequences of the *p53* transcript as described previously (chapter 2). Immunostained epidermal sheets were dehydrated and immuno-positive laser dissected mut-p53 cell clusters were lysed by proteinase K. After whole genome amplification (Genomiphi V2, GE Healthcare) of the lysate the DNA was purified by spin columns (DNeasy, QIAGEN, Venlo, The Netherlands) and served as template for PCR amplification of exons 4 – 8 using previously described primers[20]. The PCR products were completely sequenced in both directions.

Morphology and immunohistochemistry

Part of the HSEs were fixed in 4% formaldehyde, dehydrated and embedded in paraffin, whereas the other part was snap-frozen. For morphological analysis, 5µm sections were cut, deparaffinized, rehydrated and stained with haematoxylin and eosin for analysis by light microscopy. For HIF1α staining, sections (5µm) were cut, deparaffinized and rehydrated, and antigen retrieval was performed by boiling the sections in 0.1M citrate buffer (pH 6.9) in an autoclave at 110°C for 10 minutes. Subsequent steps were performed with a CSA amplification kit (Dako, ref 1500). For active-caspase-3 staining of HSE or mouse material, cryosections were cut (5µm), fixed in methanol/acetone (1:1) for 10 minutes and incubated overnight with primary antibody (anti-active-caspase-3, Ab2302, Abcam, Cambridge, UK) at 4°C. Secondary antibody (goat anti-rabbit-biotin, BA1000, Vector, Burlingame, CA) was added for 1 hour at RT and sections were stained with avidin-biotin complex (Vectastain, Vector) incubated with AEC. For *p53* staining of UV-exposed skin in mice, CM5 antibody (Monosan, Uden, The Netherlands) was used as described previously[21]. Deparaffinized sections of skin tumors from a previous study (chapter 2) were stained for mutant-p53 with Pab240 antibody as described previously[21].

Statistics

Differences in *p53* mutational spectra between the diet groups were calculated by $\chi 2$ test. Differences in the number of mut-p53 cell clusters were calculated using ANOVA. The Mann-Whitney test was used to calculate differences between percentages of cells of tumors expressing mutant p53. A P-value of <0.05 was considered as statistically significant difference. All calculations were performed with SPSS 16.0.

Results

Rapamycin alters the mutational spectrum of *p53* late in tumor development

In addition to the earlier measured altered *p53* mutational spectrum in tumors >2mm from rapamycin-fed mice (figure 2) (chapter 2), we investigated the *p53* mutations in tumors <2mm of rapamycin-fed mice from the same experiment. In a new experiment, mut-p53 cell clusters were induced in rapamycin-fed mice under the same conditions as the earlier study, and *p53* mutations in mut-p53 cell clusters were determined. Of the *p53* mutations in tumors <2mm, 80% (20 out of 25) were UV-type (i.e. C to T transition at dipyrimidine sites), and mut-p53 cell clusters contained 82% (9 out of 11) UV-type mutations (figure 2). Mut-p53 cell clusters and tumors have been previously described to harbor 79-89% UV-type mutations[12, 13]. These results show that the altered *p53* mutational spectrum in rapamycin-treated mice is only present in tumors >2mm.

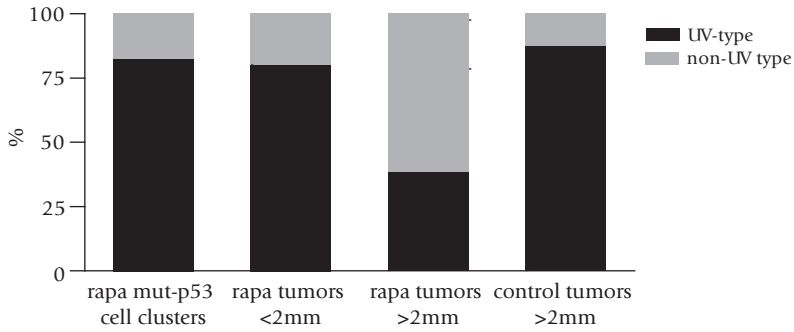

Figure 2: Percentages of UV-typical mutations (C to T transition at a dipyrimidine site) are shown here in mut-p53 cell clusters (n=15), tumors <2mm (n=21) and tumors >2mm (n=7) of rapamycin-fed mice and (n=7) of control mice (two columns for tumors >2mm from chapter 2). The mutational spectrum is only altered in tumors >2mm in rapamycin-fed mice.

Rapamycin impairs induction of mut-p53 cell clusters

In these experiments we observed fewer mut-p53 cell clusters in dorsal skin of rapamycin-treated mice than of control mice (data not shown). This may either be caused by the suppressed expression of (mutant-)p53 protein, enhanced apoptosis, or by decreased formation of mut-p53 cell clusters. To gain more insight into the mechanism, we conducted

an experiment in which mut-p53 cell clusters were induced by daily UV exposure in rapamycin-fed and control mice. Mice were put on experimental diets one week before starting UV exposures. After 10 weeks the diets were switched between the two groups. At different time points after switching food (1 to 7 days) mice were sacrificed and numbers of mut-p53 cell clusters were determined (figure 3A).

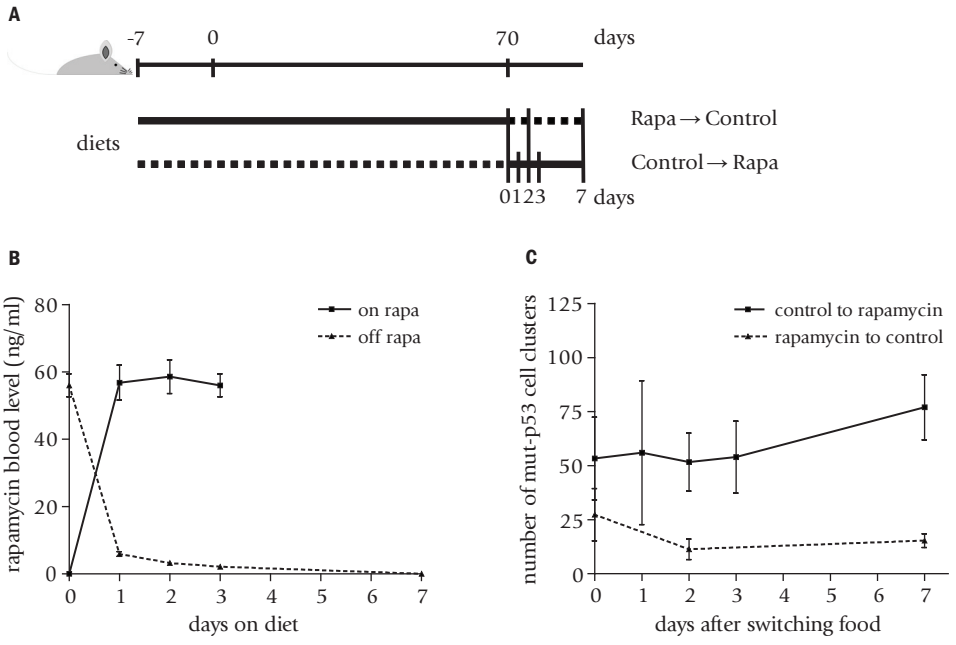

Figure 3: (**A**) Schematic presentation of the time course in the rapamycin diet cross-over experiment; daily UV exposure starts at t=0, dashed line depicts control diet and solid line diet with rapamycin, cross lines depict sampling points of skin to assess frequencies of mut-p53 overexpressing cell clusters. (**B**) rapamycin blood levels in mice started on chow containing rapamycin (solid line), and mice switching from rapamycin-containing chow to control chow (dashed line). (**C**) Numbers of mut-p53 cell clusters in epidermal sheets from mice after switching diet from rapamycin to control (dashed line) or control to rapamycin (solid line). Before switching the diets, mice were daily exposed to UV for 10 weeks. n=3-4 mice per group. Here, time point 0 refers to the time of switching diets. Error bars depict SEM.

We first measured the blood levels of rapamycin after starting or stopping rapamycin diets. Twenty-four hrs after starting the rapamycin diet, the rapamycin concentration in blood had already reached plateau levels (~57 ng/ml). When the rapamycin diet was stopped, drug

blood levels decreased to 10% of plateau after 24 hours, and were below detection limits after seven days (figure 3B).

Next, the numbers of mut-p53 cell clusters were determined in the different groups. Mice that had started on rapamycin diet during 10 weeks of UV-irradiation (n=10) harbored fewer mut-p53 cell clusters than control mice (n=10, p=0.002) Feeding of rapamycin to control mice (carrying pre-induced mut-p53 cell clusters) did not significantly change the numbers of mut-p53 cell clusters at any of the time points tested (figure 3C). Moreover, removal of rapamycin from the diet of mice did not significantly change the number of mut-p53 cell clusters at any of the selected time points (figure 3C).

Rapamycin does not affect the percentage of tumors with *p53* mutations, but does increase the mut-p53 expression in small tumors

Since the development of mut-p53 cell clusters is inhibited by rapamycin without having an effect on onset of tumors (<1mm) (chapter 2), the question arises whether mut-p53 cell clusters are genuine precursors of skin tumors. To gain more insight in the mechanisms involved, we checked whether (a proportion of) skin tumors in rapamycin-treated mice originate from cells without *p53* mutation (*p53* mutation is not obligatory for tumor formation). Therefore, we determined the percentage of tumors <2mm that contained mutations in the *p53* gene across the different groups from a previous study (chapter 2). Seventy-one percent (15 out of 21) of the tumors from mice on control diet, and 73% (11 out of 15) of the tumors from rapamycin-fed mice harbored *p53* mutations. These percentages are in agreement with a previous study[21] and show that the frequency of *p53* mutations is not different in tumors from rapamycin fed mice compared with control mice.

Expression of mutated p53 in tumors <2mm was determined by immunohistochemical staining of tumor sections. Remarkably, a higher fraction of tumor cells expressed mutated p53 in tumors of rapamycin-fed mice (n=16 from 6 mice) than in tumors of control mice (n=10 from 6 mice): 74% vs 34%, respectively, p=0.003 (figure 4). Expression of mut-p53 in tumors >2mm did not differ significantly between rapamycin-fed and control mice (89%, n=6 vs 74%, n=5, respectively).

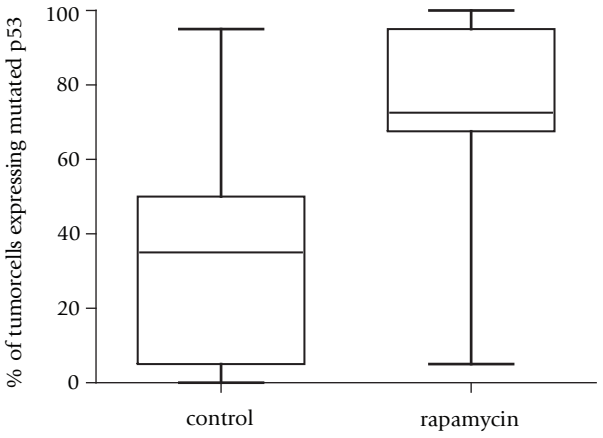

Figure 4: The fraction of mut-p53-expressing cells in tumors <2mm from rapamycin-fed mice is increased compared to the same size tumors from control mice. Staining of mutant p53 was performed on 10 and 16 tumors from six mice per group. Boxes depict upper and lower quartile and whiskers depict the minimum and maximum value.

Effect of rapamycin on active caspase-3 positivity after UV in wild-type and mutant-p53 mice

Using mice that harbor heterozygous mutations in the *p53* gene (275P>S) and littermates that were wild-type for *p53*, we investigated the effect of rapamycin on UV-induced apoptosis in exposed epidermis. Mice were fed a diet with or without admixture of rapamycin for two weeks. Subsequent exposure to 2250 J/m^2 (1.5MED for shaven mice) resulted in induction of the apoptosis marker, active caspase-3. Only mice with positive staining for mutant p53 were included in the analysis to exclude mice without cre-mediated activation of the mutant-p53 construct in the epidermis. The proportion of epidermal cells expressing active caspase-3 tended to be higher in wild-type mice (n=6) compared to mut-p53 mice (n=4) on control diet 48 hours after UV exposure (23% vs 15%, respectively, P>0.05). Rapamycin caused a slight but insignificant increase in apoptosis in wild-type mice (28%, n=6, vs 23%, n=6, respectively), whereas the increase in mutant p53 mice was two-fold, but still not significant (34%, n=4, vs 15%, n=4, respectively). As the variability in staining for apoptosis was substantial in skin samples and between mice (SD between 5 and 20%), a two-fold increase in apoptosis was not significant. Also, expression of p53 (wild-type and mutant) was determined by immunohistochemical analysis and found to be increased after UV irradiation in both mouse strains. There was no clear effect of rapamycin treatment on the fraction of cells overexpressing p53 in the irradiated skin (data not shown). The mutant p53

mice showed no baseline overexpression of mutant p53 in unirradiated (abdominal) skin, i.e. mutation of *p53* did not directly lead to overexpression of the protein.

Rapamycin enhances apoptosis in human skin equivalents (HSEs)

To assess the effect of rapamycin on apoptotic responses in human cells we performed a more elaborate dose-effect experiment using HSEs generated with cells obtained from two different human donors. The HSEs were cultured for 2 days in the presence or absence of 10nM or 100nM rapamycin. Subsequently, HSEs were irradiated with different doses of UVB (0, 30, 60, 85 and 110 mJ/cm^2), and 24 hours later HSEs were processed for assessing active caspase-3 by immunohistochemical analysis. The data shown in figure 5 clearly demonstrates that supplementation of 100nM (91 ng/ml) rapamycin to the cultures consistently results in an increased number of active caspase-3-positive cells in the basal layer of the HSEs at UV doses over 60 mJ/cm^2 (figure 5A). In addition, the number of positive cells for this apoptotic marker differed between HSEs generated with keratinocytes of the two different donors (figure 5B). Similar effects were also observed with 10nM of rapamycin (data not shown).

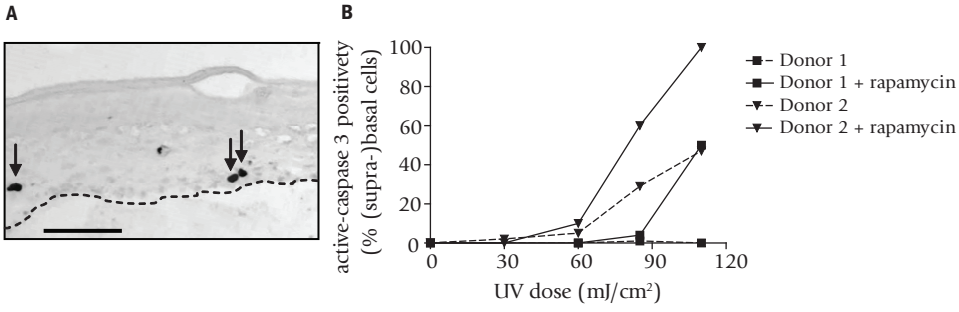

Figure 5: Effect of rapamycin on apoptosis in HSEs. (**A**) cross-section of an HSE treated with 100nM rapamycin and 24 h after irradiation with 90 mJ/cm^2 UV. The stained cells (arrows) are basal cells positive for the pro-apoptotic protein active-caspase-3. The dashed line indicates basement membrane. Scale bar=100 µm. (**B**) The percentage of positive (supra-) basal cells for active caspase-3 after UVB irradiation is increased in HSEs treated with 100nM rapamycin. Results of HSEs from two different donors are depicted. (active caspase-3+ cells in a HSE sample were counted in 2 stretches of 100 basal cells; spread in counts per HSE sample appeared to be within expected 95% confidence interval, based on a simple binomial distribution, i.e. ± 10% around 50% and ± 6% around 10% or 90%).

Rapamycin inhibits HIF1α up-regulation in HSEs after UV irradiation

Rapamycin has been shown to inhibit the accumulation of HIF1α in response to hypoxia[22]. To assess the effect of rapamycin on HIF1α induction after UV irradiation, we determined its expression after UVB irradiation using a dosage of 30 mJ/cm^2 in HSEs supplemented with or without rapamycin. The results obtained demonstrate that HSEs treated with rapamycin do not show any nuclei positive for HIF1α, while the majority of cells in control HSEs showed positive nuclei for this protein at 10 and 24 hrs after UV irradiation (figure 6A-C). The expression of HIF1α was also negative in untreated HSEs 1 hr after UV irradiation, as shown in figure 6C. Having established that HIF1α expression

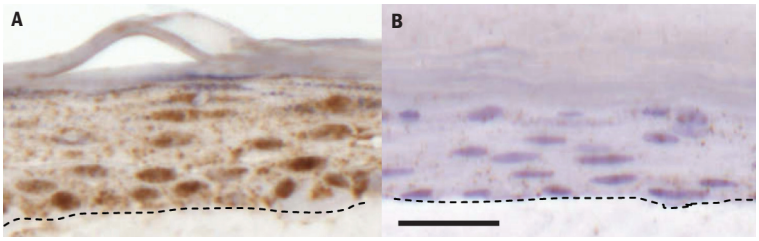

C

Time after UV-irradiation (hr)	Control	Rapamycin 100nM
1	-	-
10	++	-
24	++	-
No UV	+	-

D

UV dose (mJ/cm^2)	Control	Rapamycin 10nM	Rapamycin 100nM
60	++	-	-
85	++	-	-
110	+	-	-

Figure 6: Effect of rapamycin on HIF1α induction in HSEs after UV exposure (**A**) HIF1α-stained cross section of HSE 10 hours after irradiation with 30 mJ/cm^2 UV in the absence of rapamycin; (**B**) HIF1α-stained cross section of HSE supplemented with 100nM rapamycin 10 hours after irradiation with 30 mJ/cm^2 UV; (**C**) table on HIF1α staining at several time points after UV exposure in rapamycin-treated or mock-treated HSEs. (**D**) table on HIF1α staining at 24 hours after irradiation with different UV dosages in rapamycin-treated or mock-treated HSEs.

Legend: -=<30% positive (supra-)basal nuclei; +=50-80% positive (supra-)basal nuclei; ++=>80% positive (supra-)basal nuclei. The dashed line indicates basement membrane. Scale bar: 50 μm

in HSEs after UV exposure is upregulated after 24 h, we determined the HIF1α expression 24 h after exposing HSEs to higher UV doses (60, 85 and 110 mJ/cm^2). The different UV doses all resulted in upregulated HIF1α expression in the control samples, whereas rapamycin-treated HSEs showed fewer nuclei stained positive for HIF1α (figure 6D). In the rapamycin-treated HSEs irradiated at 85 and 110 mJ/cm^2, the staining was dispersed, possibly due to the high dose of UV irradiation that induced many disintegrated cells positive for active caspase-3.

Discussion

As rapamycin-treated mice developed UV-induced skin tumors with an altered *p53* mutational spectrum, without affecting tumor onset (chapter 2), we speculated that this altered mutational spectrum emerges late in tumor development. Our results show that putative microscopic precursor lesions and early stage tumors indeed harbored a normal UV-related *p53* mutational spectrum, and that the occurrence of an altered mutational spectrum is specific for large tumors. Since we found lower numbers of mut-p53 cell clusters in rapamycin-fed mice, we speculated that rapamycin either decreases expression of the p53 protein or acts in a pro-apoptotic manner on mut-p53 cell clusters. Our results show that rapamycin does not decrease previously induced mut-p53 cell clusters, showing neither an effect on expression of mutant p53, nor any apoptosis in the clusters. From this we conclude that rapamycin truly inhibits the formation of these cell clusters, possibly by enhanced early apoptosis. Such an enhancement of UV-induced apoptosis by rapamycin was not significant in mice in our experimental setup, but could be clearly demonstrated in more elaborate and controlled experiments in HSEs.

The type of *p53* mutations in UV-induced squamous cell carcinomas (SCCs) in mice are normally predominantly of a UV-specific type with a C>T transition on a dipyrimidine site (UV signature mutation). In a previous study (chapter 2) our group has shown that SCCs >2 mm from rapamycin-treated mice displayed an altered mutational spectrum, with a minority of UV-typical mutations. Here we showed that this shift in the type of mutations was not present in mut-p53 cell clusters and skin tumors <2mm from mice treated with rapamycin. It can therefore be concluded that the deviant *p53* mutations were either late events in the development of tumors or only a minor subset of small tumors with an altered mutational spectrum (e.g. tumors with high endogenous oxidative stress) was able to grow out into large tumors, explaining the lower yield of large tumors in rapamycin-fed mice.

Numbers of mut-p53 cell clusters were lower in mice fed rapamycin after 10 weeks of UV irradiation when compared with control mice. The number of mut-p53 cell clusters was not altered after switching the diet without rapamycin to one with rapamycin, or visa versa. Since our study showed that the number of mut-p53 cell clusters was lower when rapamycin was present during UV exposure, and that the number of mut-p53 cell clusters was not decreased after introduction of rapamycin, it can be surmised that rapamycin does not suppress mut-p53 expression or force mut-p53 cell clusters into apoptosis, but genuinely inhibits the formation of mut-p53 cell clusters. This might be attributable to an enhancement of UV-induced apoptosis of DNA damaged cells, thus preventing (*p53*) mutation appearance (see below).

Tumor latency times in UV-irradiated hairless mice were not affected by rapamycin (chapter 2), but rapamycin in the present study impaired formation of mut-p53 cell clusters. This is an interesting finding since previous studies have correlated tumor induction closely with that of mut-p53 cell clusters[12, 23]. The present study shows for the first time that a drug can impair the development of mut-p53 cell clusters without affecting tumor onset. For various reasons mut-p53 cell clusters have previously been considered precursor lesions for skin tumors[12, 21], an assumption that is challenged by this study. It is still likely that most SCCs develop out of mut-p53 cell clusters since mutation of the *p53* gene appears to be a consistent early event in squamous cell carcinoma development, i.e. already present in a majority of precursor lesions and subsequently in a majority of SCCs[11, 21]. But it is now clear that numbers of the p53-mut cell clusters cannot be reliably used as indicator for tumor risk. Since the large majority of mut-p53 cell clusters do not develop into tumors[12], the impaired induction by rapamycin may only affect a majority of mut-p53 cell clusters which are not genuine precursors of tumors (actinic keratoses and SCCs). Hypothetically, a small specific subset of mut-p53 cell clusters might not be inhibited by rapamycin, e.g. due to an additional oncogenic change, and constitute the sole true precursors of the tumors. However, this additional oncogenic change remains to be identified and requires further study.

The percentage of small tumors harboring a mutation in the *p53* gene was not different between the mice on rapamycin and control diet, indicating that mutation of *p53* remained an important early event in the tumors in the rapamycin-treated group. It should, however, be noted that the small tumors were harvested at the end of the experiment and the skin of mice harbored many mut-p53 cell clusters at that time. This would make it more likely for a tumor to start with a mutated *p53* by chance, since many epidermal cells harbor a mutated *p53* in that stage of the experiment. A higher fraction of tumor cells expressed mutated p53 in

tumors <2mm after rapamycin-treatment of mice, compared to the same small-sized tumors of control mice. Rapamycin had, however, no apparent effect on the tumor development at that stage. This difference in expression of mutant p53 between rapamycin-fed mice and controls was not observed in tumors >2mm.

Rapamycin did not significantly alter the apoptotic response or p53 expression in wild-type mice or mice harboring a germline *p53* mutation. After a single dose of UV the active caspase-3 positive cell fraction in the epidermis of skin cells from mice on rapamycin diet was higher than in mice on control diet, especially in mut-p53 mice, but these rapamycin effects were not significant.. The variability in the staining for active caspase-3 (and p53) appeared to have prevented us from observing significant increases by rapamycin. Nonetheless, in more elaborate and controlled experiments in HSEs we did find a clear increase in UV-induced apoptosis by rapamycin. We found associated HIF1α accumulation in keratinocytes after UV exposure of human skin equivalents to be inhibited by rapamycin. Previously it has been shown that HIF1α is upregulated after hypoxia[24] and UV irradiation[6, 25], and that rapamycin can prevent hypoxia-induced HIF1α accumulation[22]. Here we show a similar effect of rapamycin on UV-induced HIF1α accumulation. HIF1α has been reported to inhibit or induce apoptosis, depending on the cell type[26, 27]. Our data suggest that HIF1α likely moderates UV-induced apoptosis, and that rapamycin neutralizes this HIF1α effect. Early rapamycin-enhanced apoptosis in UV-damaged cells may have reduced the number of p53-mut clusters that develop. Moreover, our previous finding that rapamycin inhibits the development of large tumors (chapter 2) might be attributable to attenuating the HIF1α pathway, thereby impairing the rate at which small tumors grow.

A recent prospective, controlled, clinical trial showed that transplant recipients who were switched to rapamycin treatment had a reduced rate of (pre)malignancies and nonmelanoma skin cancer[3]. In relation to this trial, the present study shows that rapamycin affects specific processes that may play a role in skin tumorigenesis.

To summarize, after UV irradiation apoptosis is increased and HIF1α accumulation is impaired in a human skin model. In our experimental setup we could however not measure such an effect of rapamycin on UV-induced apoptosis in freely moving mice, but rapamycin did reduce mut-p53 cell cluster formation in chronically UV-exposed mice. Although this rapamcyin-related reduction in mut-p53 cell clusters did not result in a reduced onset of tumors, rapamycin treatment did reduce the number of larger tumors. Besides providing insight on the precise impact rapamycin has on UV responses and UV carcinogenesis,

our data unexpectedly demonstrated that fewer mut-p53 cell clusters do not necessarily correspond with a reduced onset of tumors.

Acknowledgements

We thank prof. R. Fodde under whose supervision HJvK generated the LSL-p53$^{P275S/+}$ mice, and dr. E. Robanus Maandag for maintaining this mouse strain and the EIIa-Cre deleter mice, and making them available.

References

1. Ingvar A, Smedby KE, Lindelöf B, Fernberg P, Bellocco R, Tufveson G, Höglund P, Adami J. Immunosuppressive treatment after solid organ transplantation and risk of post-transplant cutaneous squamous cell carcinoma. Nephrology, Dialysis, Transplantation: Official Publication of the European Dialysis and Transplant Association European Renal Association 2010;25:2764-71.
2. Dantal J, Hourmant M, Cantarovich D, Giral M, Blancho G, Dreno B, Soulillou JP. Effect of long-term immunosuppression in kidney-graft recipients on cancer incidence: randomised comparison of two cyclosporin regimens. Lancet 1998;351:623-8.
3. Salgo R, Gossmann J, Schöfer H, Kachel HG, Kuck J, Geiger H, Kaufmann R, Scheuermann EH. Switch to a Sirolimus-Based Immunosuppression in Long-Term Renal Transplant Recipients: Reduced Rate of (Pre-)Malignancies and Nonmelanoma Skin Cancer in a Prospective, Randomized, Assessor-Blinded, Controlled Clinical Trial. American Journal of Transplantation 2010.
4. Hollander MC, Blumenthal GM, Dennis PA. PTEN loss in the continuum of common cancers, rare syndromes and mouse models. Nat Rev Cancer 2011;11:289-301.
5. Guba M, von Breitenbuch P, Steinbauer M, Koehl G, Flegel S, Hornung M, Bruns CJ, Zuelke C, Farkas S, Anthuber M, Jauch K-W, Geissler EK. Rapamycin inhibits primary and metastatic tumor growth by antiangiogenesis: involvement of vascular endothelial growth factor. Nat Med 2002;8:128-35.
6. Wunderlich L, Paragh G, Wikonkal NM, Banhegyi G, Karpati S, Mandl J. UVB induces a biphasic response of HIF-1alpha in cultured human keratinocytes. Experimental Dermatology 2008;17:335-42.
7. Huang S, Liu LN, Hosoi H, Dilling MB, Shikata T, Houghton PJ. p53/p21CIP1 Cooperate in Enforcing Rapamycin-induced G1 Arrest and Determine the Cellular Response to Rapamycin. Cancer Res 2001;61:3373-81.
8. Wulff BC, Kusewitt DF, VanBuskirk AM, Thomas-Ahner JM, Duncan FJ, Oberyszyn TM. Sirolimus Reduces the Incidence and Progression of UVB-Induced Skin Cancer in SKH Mice even with Co-administration of Cyclosporine A. J Invest Dermatol 2008;128:2467-73.
9. de Gruijl FR, Koehl GE, Voskamp P, Strik A, Rebel HG, Gaumann A, de Fijter JW, Tensen CP, Bavinck JN, Geissler EK. Early and late effects of the immunosuppressants rapamycin and mycophenolate mofetil on UV carcinogenesis. Int J Cancer 2010;127:796-804.
10. Neklesa TK, Davis RW. Superoxide anions regulate TORC1 and its ability to bind Fpr1:rapamycin complex. Proceedings of the National Academy of Sciences of the United States of America 2008;105:15166-71.
11. Jonason AS, Kunala S, Price GJ, Restifo RJ, Spinelli HM, Persing JA, Leffell DJ, Tarone RE, Brash DE. Frequent clones of p53-mutated keratinocytes in normal human skin. Proc Natl Acad Sci U S A 1996;93:14025-9.
12. Rebel H, Kram N, Westerman A, Banus S, van Kranen HJ, de Gruijl FR. Relationship between UV-induced mutant p53 patches and skin tumours, analysed by mutation spectra and by induction kinetics in various DNA-repair-deficient mice. Carcinogenesis 2005;26:2123-30.

13. Kramata P, Lu Y-P, Lou Y-R, Singh RN, Kwon SM, Conney AH. Patches of Mutant p53-Immunoreactive Epidermal Cells Induced by Chronic UVB Irradiation Harbor the Same p53 Mutations as Squamous Cell Carcinomas in the Skin of Hairless SKH-1 Mice. Cancer Res 2005;65:3577-85.

14. Ren ZP, Ponten F, Nister M, Ponten J. Two distinct p53 immunohistochemical patterns in human squamous-cell skin cancer, precursors and normal epidermis. Int J Cancer 1996;69:174-9.

15. Olive KP, Tuveson DA, Ruhe ZC, Yin B, Willis NA, Bronson RT, Crowley D, Jacks T. Mutant p53 gain of function in two mouse models of Li-Fraumeni syndrome. Cell 2004;119:847-60.

16. de Vries A, Flores ER, Miranda B, Hsieh H-M, van Oostrom CTM, Sage J, Jacks T. Targeted point mutations of p53 lead to dominant-negative inhibition of wild-type p53 function. Proceedings of the National Academy of Sciences of the United States of America 2002;99:2948-53.

17. Tuveson DA, Shaw AT, Willis NA, Silver DP, Jackson EL, Chang S, Mercer KL, Grochow R, Hock H, Crowley D, Hingorani SR, Zaks T, et al. Endogenous oncogenic K-ras(G12D) stimulates proliferation and widespread neoplastic and developmental defects. Cancer Cell 2004;5:375-87.

18. El-Ghalbzouri A, Gibbs S, Lamme E, Van Blitterswijk CA, Ponec M. Effect of fibroblasts on epidermal regeneration. Br J Dermatol 2002;147:230-43.

19. Krotz F, Keller M, Derflinger S, Schmid H, Gloe T, Bassermann F, Duyster J, Cohen CD, Schuhmann C, Klauss V, Pohl U, Stempfle H-U, et al. Mycophenolate Acid Inhibits Endothelial NAD(P)H Oxidase Activity and Superoxide Formation by a Rac1-Dependent Mechanism. Hypertension 2007;49:201-8.

20. van Kranen HJ, Westerman A, Berg RJW, Kram N, van Kreijl CF, Wester PW, de Gruijl FR. Dose-dependent effects of UVB-induced skin carcinogenesis in hairless p53 knockout mice. Mutation Research 2005;571:81-90.

21. Berg RJ, van Kranen HJ, Rebel HG, de Vries A, van Vloten WA, Van Kreijl CF, van der Leun JC, de Gruijl FR. Early p53 alterations in mouse skin carcinogenesis by UVB radiation: immunohistochemical detection of mutant p53 protein in clusters of preneoplastic epidermal cells. Proceedings of the National Academy of Sciences 1996;93:274 -8.

22. Hudson CC, Liu M, Chiang GG, Otterness DM, Loomis DC, Kaper F, Giaccia AJ, Abraham RT. Regulation of Hypoxia-Inducible Factor 1α Expression and Function by the Mammalian Target of Rapamycin. Molecular and Cellular Biology 2002;22:7004-14.

23. Rebel H, Mosnier LO, Berg RJW, Vries AW-d, van Steeg H, van Kranen HJ, de Gruijl FR. Early p53-positive Foci as Indicators of Tumor Risk in Ultraviolet-exposed Hairless Mice: Kinetics of Induction, Effects of DNA Repair Deficiency, and p53 Heterozygosity. Cancer Res 2001;61:977-83.

24. Wang GL, Jiang BH, Rue EA, Semenza GL. Hypoxia-inducible factor 1 is a basic-helix-loop-helix-PAS heterodimer regulated by cellular O2 tension. Proceedings of the National Academy of Sciences of the United States of America 1995;92:5510-4.

25. Rezvani HR, Dedieu S, North S, Belloc F, Rossignol R, Letellier T, de Verneuil H, Taieb A, Mazurier F. Hypoxia-inducible Factor-1{alpha}, a Key Factor in the Keratinocyte Response to UVB Exposure. J. Biol. Chem. 2007;282:16413-22.

26. Piret JP, Mottet D, Raes M, Michiels C. Is HIF-1alpha a pro- or an anti-apoptotic protein? Biochem Pharmacol 2002;64:889-92.

27. Greijer AE, van der Wall E. The role of hypoxia inducible factor 1 (HIF-1) in hypoxia induced apoptosis. Journal of Clinical Pathology 2004;57:1009-14.